Mechanism of submonolayer oxide formation on silicon surfaces upon thermal oxidation

V. D. Borman, E. P. Gusev, Yu. Yu. Lebedinski, and V. I. Troyan
Moscow Engineering Physics Institute, Moscow 115409, Russia
(Received 16 June 1992; revised manuscript received 27 September 1993)

We present the results of an experimental and theoretical investigation of the initial oxidation of Si(100). Oxidation kinetics were measured in real time by x-ray-photoelectron spectroscopy. In the pressure and temperature regime studied, we observed the following kinetic phenomena: a decrease of the initial oxidation rate with increasing temperature, kinetic curves (i.e., coverage vs time) showing saturation with the saturation value increase for the higher temperatures, and a transition from "passive" to "active" oxidation. To account for the experimental results a phenomenological first-order phase-transition theory was used. On comparing the experimental and theoretical results, we suggested a physical mechanism for submonolayer silicon oxide formation.

I. INTRODUCTION

The interaction of oxygen with the silicon surface is of great interest from both a fundamental viewpoint and numerous technological applications.[1-4] However, despite many publications on the initial oxidation,[5-11] a reasonable physical mechanism of submonolayer oxide formation has yet to be proposed. The main aim of this paper is to elucidate the mechanism of high-temperature initial silicon oxidation.

Following a brief discussion of the experimental setup and coverage calibration procedures (Sec. II) we review our main experimental results on the kinetics of submonolayer oxide growth (Sec. III). Conventionally, oxidation kinetics are measured in a point-by-point manner[5,8] (heating, exposing, pumping, cooling, then measuring). Unfortunately, both surface oxygen concentration and oxygen (silicon) atom states may change during this process; it is quite possible that the system changes between the elevated and ambient temperature.[9,12] That is why in the present work we use a real-time method[12,13] for silicon oxidation. The basic kinetic properties (such as coverage saturation and the decrease in oxidation rate with increasing temperature) appear (Sec. III) to agree qualitatively with the results obtained using point-by-point methods. Our method, however, reveals new features. In particular, the characteristic oxide formation time at $T > 1000$ K was found to be comparable to the mean lifetime of oxygen atoms on the surface. We also observed a change in photoelectron spectra at these temperatures that could be caused by oxygen atom diffusion into the silicon crystal.

In our recent x-ray photoelectron (XPS) study[12] of Si^{n+}-state[14] accumulation during high-temperature initial silicon oxidation, it was demonstrated that submonolayer silicon oxide is formed by a first-order phase-transition process. Such an interpretation is supported (Sec. IV A) by the following experiment facts: the existence of critical oxygen exposure ϵ_c,[15] critical coverage θ_c,[10] and a critical oxygen pressure p_c;[7,16-20] formation of oxide islands[5,7,8,11,15,19-25] distinct from an adsorbed phase; and coexistence of the adsorbed phase and oxide phase during surface oxide growth.[10,21,24,26] Therefore, we have presented a phenomenological theory of first-order phase transitions[27,28] (Sec. IV B) in order to explain the experimental results. We studied the general case of oxide island growth. Then we considered several limiting cases that depend on (i) the relationship between the oxygen delivery time and the phase transformation time, and (ii) a mechanism of oxygen delivery to the island (by direct impingement or surface diffusion). Finally, among all possible cases we found the one responsible for silicon oxide growth. The theory has an advantage when compared to known models of the nucleation and new phase island growth[29] (e.g., the models suggested in Refs. 30 and 31), since it takes into consideration island growth in nonequilibrium conditions when a new phase grows during oxygen adsorption from the gas phase, i.e., the concentration of adatoms on the surface is nonconservative, the finite time of the phase transformation,[32] and oxide island interactions. It was these circumstances that allowed us (Sec. IV C) to describe the experimental results.

By comparing the experimental and theoretical results, we suggest (Sec. IV C) a physical mechanism of silicon oxide growth. According to the proposed mechanism, the high-temperature growth of surface oxide islands is due to oxygen delivery via surface diffusion of adsorbed oxygen. There is a potential barrier for oxygen adatoms to incorporate into the island at the island perimeter. This incorporation process is the limiting step of initial silicon oxidation. The mechanism is shown to describe the experimental data (both ours and those published previously) on the kinetics of surface oxidation, i.e., the dependence of oxide coverage upon oxidation time, temperature and pressure, existence of the critical pressure, and transition from so-called active oxidation to passive oxidation. We also explain the recently observed[8] deviation in the coverage vs exposure ϵ ($\epsilon = pt$) dependence from the conventional behavior,[30] i.e., when oxide coverage does not depend simply on exposure, but is determined by pressure and time separately. Such an explanation is impossible within the framework of the known models.[29-31]

0163-1829/94/49(8)/5415(9)/$06.00

II. EXPERIMENT

A. Experimental setup

The experiments were carried out in the XSAM-800 (Kratos) system. A Mg $K\alpha$ source was used for XPS; the energy resolution and accuracy were 0.9 and 0.1 eV, respectively. The binding energy (E_{be}) was calibrated with respect to the C 1s line ($E_{be}=284.6$ eV). The cleaning of the silicon surface [p-type Si(100)] included chemical etching just before sample loading into the analyzer chamber followed by cycling of ion (Ar^+, 3.5 keV) bombardment and UHV annealing (10^{-9} Torr, 1100 K). Such a treatment results in an atomically clean surface within the sensitivity of the XPS and Auger electron spectroscopy. In order to provide measurements at temperatures up to 1200 K we designed a custom heater. In this construction, the sample was heated by flowing a current through a thin U-shaped gold resistor deposited on a ceramic substrate. The Si sample was fastened to the ceramic substrate. It should be noted that the use of XPS and our custom heater allowed us to avoid problems of oxidation stimulated by the electron beam[33] or by excited oxygen.[34]

The experiments on the initial oxidation kinetics were carried out in the following sequence: (1) surface cleaning, as described above; (2) sample heating to a certain temperature (800–1200 K); (3) recording of O 1s XPS intensity (I_O) vs time (t) in real time simultaneously with oxygen admission into the analyzer chamber (oxygen pressure of 10^{-6} Torr) (we recorded the intensity I_O at the O 1s line maximum in the low-resolution mode; this permits a determination of the net concentration of surface oxygen); (4) after oxidation for 10 min [or exposure of 600 L (1 L$=10^{-6}$ Torr s)], oxygen admission was stopped. At the end of the $I_O(t)$ curve measurement, detailed O 1s and Si 2p spectra in high-resolution mode were examined to identify the "final" states of oxygen and silicon. Details of the real-time experiments have been published elsewhere.[12,13]

B. Oxygen-coverage calibration

To connect the oxygen (I_O) and silicon (I_{Si}) signals with surface oxygen concentration (or coverage), we used the following method. The method is based on the Si 2p intensity attenuation during oxygen interaction with the surface. For submonolayer coverages, the effective thickness of the oxygen layer is substantially less than Si 2p photoelectron escape depth in oxide, λ_{ox}, and one can consider that the intensity of I_{Si} decreases linearly with θ:

$$I_{Si}=I_{Si}^{O}(1-\mu\theta) . \tag{1}$$

Here, $\theta=n_O/n_s$ is the coverage, n_O is the surface oxygen concentration, n_s is the density of surface silicon, μ is a coefficient that reflects substrate signal attenuation by the oxide layer ($\mu=d_m/\lambda_{ox}$, where d_m is the thickness of the oxide monolayer), and I_{Si}^{O} is the Si 2p photoelectron intensity corresponding to the clean surface:

$$I_{Si}^{O}=T(E_{Si})C_{Si}\sigma_{Si}\lambda_{Si}\cos\beta . \tag{2}$$

$T(E_{Si})$ is the transmission function of the spectrometer, E_{Si} is the kinetic energy of the Si 2p photoelectrons, λ_{Si} is the photoelectron escape depth in silicon, C_{Si} is the silicon volume concentration, σ_{Si} is the Si 2p photoionization cross section, and β is the angle between the sample normal and the analyzer. By measuring the intensities of I_{Si} and I_{Si}^{O}, coverage can be easily calculated as

$$\theta=(1-I_{Si}/I_{Si}^{O})/\mu . \tag{3}$$

The unknown coefficient μ can be determined as follows. On dividing the intensity of I_{Si} (1) by the corresponding submonolayer oxygen intensity of $I_O=T(E_O)\sigma_O n_O$ (σ_O—O1s core-level photoionization cross section) and taking into account (2), we find that

$$I_{Si}/I_O=I_{Si}^{O}/I_O-\kappa;\quad \kappa=\mu\frac{T(E_{Si})\sigma_{Si}C_{Si}\lambda_{Si}\cos\beta}{T(E_O)\sigma_O n_s} . \tag{4}$$

The parameter of κ was determined by a simultaneous recording of the oxygen (I_O) and silicon (I_{Si}) intensities during oxygen exposure at $T=1130$ K. Based on this result, we plotted the dependence of I_{Si}/I_O versus I_O^{-1} (Fig. 1). As can be seen in Fig. 1, the experimental points belong to a straight line. The slope fits well with the known value of I_{Si}^{O}. Such behavior takes place in accordance with Eq. (4), proving the reliability of the calibration method. The value of $\kappa=0.44$ was determined from the intersection of the line with the y axis (Fig. 1). Using this value of κ, we calculate the coefficient μ from (4). For this, we have used the following values: $\sigma_O=2.85\sigma_{C\,1s}$, $\sigma_{Si}=0.573\sigma_{C\,1s}$ (Mg $K\alpha$ source, $\sigma_{C\,1s}$ is the cross section[35] of the 1s core level of carbon),[36] $\lambda_{Si}=13$ Å,[37] $C_{Si}=4.99\times10^{22}$ cm^{-3}, $n_s=6.8\times10^{14}$ cm^{-2} [for Si(100)], $\cos\beta=1$, and $T(E_k)\sim E_k$ (in the FRR regime). Substitution of these values into Eq. (4) gives rise to $\mu=0.14$. Finally, this value of μ is used to determine the coverage of θ on the basis of the intensity of I_{Si} [according to Eq. (3)] or corresponding oxygen intensity I_O (see, for example, Fig. 3). Using $\mu=0.14$ and $\lambda_{ox}=21$

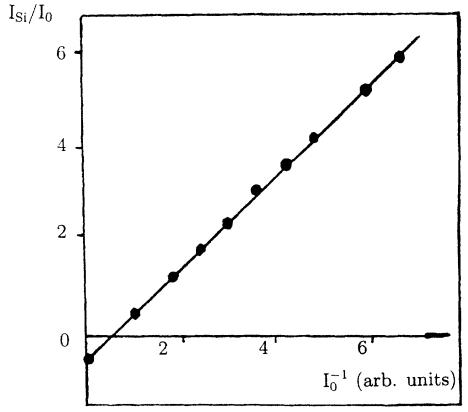

FIG. 1. The dependence of the ratio of silicon (I_{Si}) and oxygen (I_O) intensities upon inverse oxygen intensity.

Å,[37] we obtain a realistic value of the monolayer oxide thickness of $d_m = 3$ Å.

It should be mentioned that this calibration method permits us to determine oxygen coverage immediately at the experiment and without reference samples or additional methods for surface analysis. We have used this method previously to calculate coverages during oxygen-on-nickel experiments.[27] The results were found to agree with a calibration obtained by nuclear-reaction analysis,[38] an "absolute" coverage method.

III. RESULTS

In order to determine the oxygen and silicon states during the initial oxidation, high-resolution spectra of the Si 2*p* and O 1*s* lines were examined. It was found[39] that there were four states of silicon atoms near the surface. Comparison between the Si 2*p* spectra corresponding to the clean surface [Fig. 2(a)] and exposed surface [Fig. 2(c)] shows that the latter exhibits a shoulder at higher binding energies relative to the substrate Si 2*p* peak (99 eV). This shoulder is due to[5,9–12,39] silicon atoms in different oxidation states: Si^{1+}, Si^{2+}, Si^{3+}, and Si^{4+}. The decomposition of the Si 2*p* spectrum into the components was shown, for instance, in Fig. 1 of Ref. 12 (see also Ref. 11).

Now we discuss the O 1*s* spectra that we use to record the oxidation kinetics. Hollinger *et al.*[26] observed two oxygen states. The main peak at 532.3±0.3 eV was suggested to correspond to an oxidelike bridging oxygen, and the additional peak at 533.8 eV to the atomic nonbridging oxygen. Morgen *et al.*[40] also observed a shoulder which was located from 0.5 to 3.5 eV higher in energy relative to the main peak at 532.1 eV. However, they interpreted this feature as a satellite structure of the O 1*s* spectrum. Such an interpretation was subsequently criticized in Ref. 41, where it was proved that the high-energy component was actually due to atomic nonbridging oxygen. Two oxygen species,[42] bridging and nonbridging, on silicon surfaces were observed recently by scanning tunneling microscopy (STM).[22]

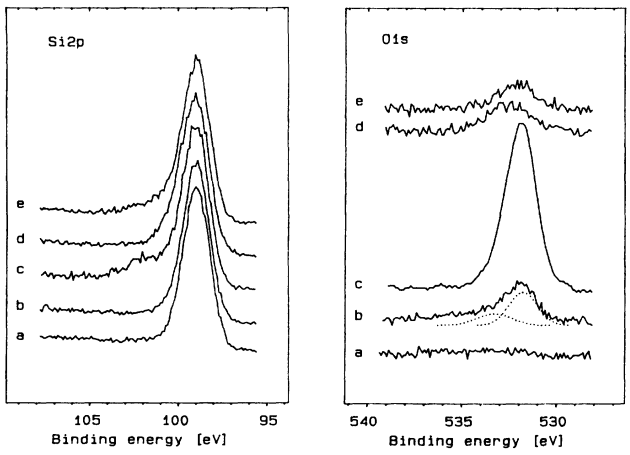

FIG. 2. Si 2*p* normalized (left) and O 1*s* (right) photoelectron spectra. (a) Clean surface; (b) exposed at room temperature, $\epsilon = 600$ L, 1 L $= 10^{-6}$ Torr s, ($\theta = 0.4$); (c) exposed at $T = 1020$ K, $\epsilon = 600$ L ($\theta = 1.3$); (c) and (d) followed by UHV annealing for 10 min at $T = 1020$ K; (e) exposed at 1090 K, $\epsilon = 600$ L.

We also observed the shoulder along with the main peak at 531.7 eV at $T = 300$ K [Fig. 2(b)]. A least-squares decomposition of the O 1*s* spectrum into two Gaussian components shows that the shoulder consists of a peak at 533.5 eV with an intensity approximately four times less than the main peak. According to the interpretation of Hollinger *et al.*,[26] these two peaks at 531.7 and 533.5 eV most likely correspond to an oxidelike bridging oxygen and an atomic nonbridging oxygen species, respectively. The Si 2*p* spectrum [Fig. 2(b)] corresponding to these room-temperature exposures is similar to the spectrum of the clean surface with very small intensities of Si^{1+} and Si^{2+} states. In other words, the "true" oxide state (i.e., Si^{4+}) does not appear at $T = 300$ K and relatively low exposures. At elevated temperatures, the O 1*s* spectrum represents almost symmetric peaks at 531.8 eV with a small wing on the high-binding-energy side of the peak [Fig. 2(c)]. Simultaneously, Si^{3+} and Si^{4+} states appear in the Si 2*p* spectrum [Fig. 2(c)]. These results are consistent with the data published previously.[26,40,41] However, the maximum temperature achieved in the earlier experiments was only ~775 K,[26] where no oxygen leaving the surface could be detected.

A quite different situation occurs at temperatures greater than 1000 K. Clean silicon was exposed to oxygen ($\epsilon = 600$ L) at $T = 1020$ K [Fig. 2(c)] and annealed for 10 min at the same temperature [Fig. 2(d)]. It is clearly seen from the Si 2*p* spectrum [Fig. 2(d)] that the shoulder disappears and the intensity of the main peak at 99 eV increases. The annealing transformed the O 1*s* spectrum as well: (i) peak intensity decreased by a factor of 4.7 and (ii) the position of the line maximum was shifted by 0.4 eV to $E_{be} = 532.4$ eV, which reflected the appearance of a new oxygen state. Moreover, this state could not be connected with the oxide states due to lack of the shoulder in the Si 2*p* spectrum. It is important to note that the position of this peak differs from the peak position of the bridging (531.8 eV) and nonbridging (533.5 eV) oxygen. This fact may be connected with the puckered, bond-centered interstitial position of oxygen atoms that have diffused into silicon.[43–45] The electronic state of oxygen in Si-O-Si bridge sites and in interstitial sites seems to be different as noted by the shifted O 1*s* core-level energies. Therefore, we assume that the O 1*s* peak with $E_{be} = 532.4$ eV [Fig. 2(d)] corresponds to the oxygen atoms that have diffused into the subsurface region. The known high value of the oxygen-in-silicon diffusion activation energy [2.53 eV (Refs. 43–45)] can explain why Hollinger *et al.*[26] did not observe the diffusion of oxygen into the subsurface region at moderate (< 775 K) temperatures.

The kinetics of oxygen uptake during the initial oxidation is depicted in Fig. 3. The following features should be noted. First, the kinetic curves (1–3) tend to a saturation at $t > 200c$. Additional exposure leads to the saturation of curve 4 as well. Second, the value of coverage at the saturation increases with increasing temperature. Third, the rate of oxidation K ($= d\theta/dt$) decreases anomalously with increasing temperature with an effective "ac-

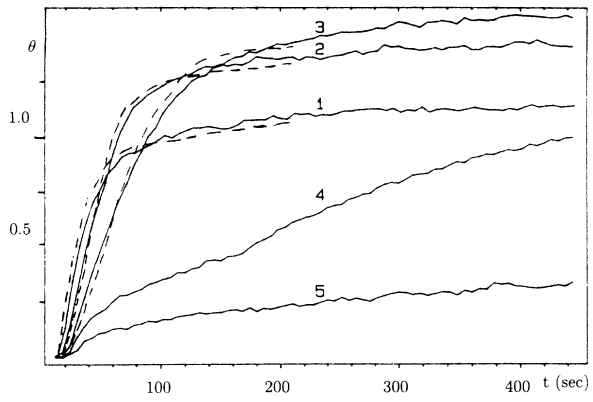

FIG. 3. Oxygen coverage vs exposure time at $T=970$ K (1), 1050 K (2), 1110 K (3), 1150 K (4), 1190 K (5). Solid line, experiment; dashed line, least-squares fitting by using formula (7). The corresponding theoretical parameters are $C_1=1.05$, $C_2=3.8\times10^{-2}$ sec^{-1} (970 K); $C_1=1.3$, $C_2=2.3\times10^{-2}$ sec^{-1} (1050 K); $C_1=1.4$, $C_2=1.1\times10^{-2}$ sec^{-1} (1110 K).

tivation" energy of $E_a=-2.3$ eV. Unlike curves 1–4, curve 5 exhibits not only an extremely low rate of oxygen uptake, but also the absence of a Si^{4+} state [Fig. 2(e)] after exposition for 10 min ($\epsilon=600$ L) according to a deconvolution of the Si 2p photoelectron spectrum. As to the O 1s spectrum [Fig. 2(c)] recorded after oxidation for 10 min for curves 1–3, the deconvolution shows that the main state is the oxidelike bridging oxygen, whereas the contributions of the other two states at this temperature do not exceed 10%. This means that although the kinetic curves $\theta(t)$ formally reflect the accumulation of all forms of oxygen, the actual concentration of the atomic nonbridging oxygen and subsurface oxygen is negligible.

As mentioned above, a decrease of surface oxygen concentration takes place during UHV annealing. We now discuss this process in more detail. Annealing for 10 min yields a 90% decrease in surface oxygen concentration (Fig. 4). Hence, the characteristic time for oxygen to leave the surface at elevated temperatures appears to be comparable to the time of oxide formation (cf. Fig. 3). This fact implies that in any theoretical model of the initial oxidation of silicon, it is necessary to consider the process of oxygen disappearance from the surface.

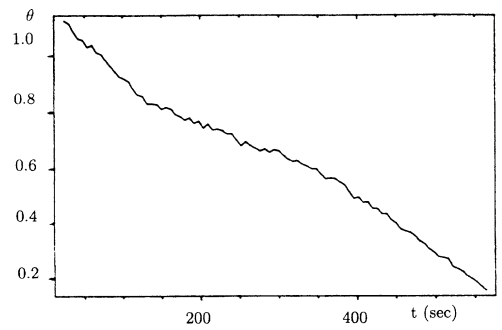

FIG. 4. Kinetics of oxygen coverage during UHV annealing at $T=1020$ K. The sample was exposed to oxygen for 10 min before annealing.

Second, this result clearly shows the advantage of a real-time method for kinetic measurements, especially at high temperatures. There are two possible channels for oxygen to leave the surface: diffusion into the bulk and/or desorption in the form of SiO.[7,16] Mass-spectrometry analysis[7] has shown that oxygen itself is not desorbed up to 1400 K. Unfortunately, we could not distinguish between these channels on the basis of the results obtained in the experiment. We can say only that the appearance of an additional O 1s peak with $E_{be}=532.4$ eV [Fig. 2(d)] implies that diffusion into the bulk could occur. As for the desorption channel, SiO is known[7] to desorb in the temperature range (975–1400 K) examined in our work.

IV. DISCUSSION

A. Formation of a submonolayer oxide on the silicon surface as a first-order phase transition

Based on the result of recent experiments,[5,7,8,11,15,19–25] one may conclude that the oxide phase on the silicon surface at $\theta<1$ grows in the form of islands. In particular, Tabe *et al.*[5] found using soft XPS that some silicon atoms were oxidized faster than others (i.e., had more oxygen atoms bonded to them) during the initial oxidation of Si(111) 7×7 at high temperatures, so that the distribution of oxygen atoms on the surface was highly nonuniform. Taking into account this observation and the results of an O 1s spectrum analysis, they suggested that nonuniform oxidation with microscopic phase separation of SiO_2 and Si regions occurred during the initial stages of oxygen interaction with the Si(111) surface. At $T>875$ K, valence spectra during initial oxidation of Si(100) (Ref. 8) showed a peak corresponding to the surface states at $\theta>1$. Thus, the authors of this work concluded that initially oxidized surfaces at high temperatures ($T>875$ K) and low pressures could be understood as a juxtaposition of SiO_2-like regions and bare silicon areas. Himpsel *et al.*[11] investigated the structure of the Si/SiO_2 interface by high-resolution photoelectron spectroscopy. For very thin oxide films (8 Å or less) the intensity of Si^{1+}, Si^{2+}, Si^{3+} states was found to decrease relative to the bulk line although their distribution remained unchanged. They postulated that these films were not continuous (i.e., islandlike), giving rise to extra emission from clean silicon through pinholes. The results of an investigation of silicon oxidation at $T=975$ K by molecular-beam[7] techniques showed the presence of bare silicon areas even at relatively high coverages ($\theta\geq1$). SiO_2 island growth mode may also be related to the microcrystalline growth (with 100–200-Å lateral size) in the initial regime observed by high-resolution transmission electron microscopy[21] for oxide films grown on Si(100) at $T=1080$ K. Clustering on silicon surfaces during initial oxidation was observed directly by STM.[15,22–25]

It is worthwhile to note that surface oxide formation exhibits a threshold character, i.e., the oxide starts to grow only after approaching a critical value of exposure[15] or oxygen concentration.[10] One may conclude from an analysis of the results of Hollinger and Himpsel[10] that the critical oxygen coverage is $\theta_c=0.2$. Related to the criti-

cal exposure and critical coverage, a temperature-dependent critical oxygen pressure (p_c) was observed in Refs. 16 and 17. At $p > p_c$, an oxide phase forms (passive oxidation), whereas at $p < p_c$ surface etching (active oxidation) occurs because of volatile SiO.[7,16,18–20,46] One more input needed to help in the interpretation of surface oxide formation as a first-order phase transition is the coexistence of absorbed and oxide phases during the initial stages of silicon[10,12,22,24,26] oxidation.

Summing up the results (Table I), it should be emphasized that the formation and growth of the oxide islands, the threshold character of the oxide formation (i.e., the existence of a critical coverage, critical exposure, and critical pressure), the coexistence of adsorbed and oxide phases, strongly supports the validity of the interpretation of oxide formation as a first-order phase transition.

B. The kinetics of oxide phase formation on solid surfaces within the framework of a phenomenological theory of first-order phase transitions

Starting from the argument that submonolayer oxide formation occurs as a first-order phase transition, we recently[27,28] proposed a general approach to describe surface oxide growth. We report here only the main ideas of this phenomenological theory of oxide island growth at $\theta < 1$ and present the equation for oxide coverage, $\theta_{ox}(p,t,T)$, which will be employed below (Sec. IV C) to account for the initial silicon oxidation.

Growth of two-dimensional[47] oxide islands occurs in two stages.[27,28] The first is associated with oxygen delivery to the growing island by means of surface diffusion or/and direct impingement of O_2 from the gas phase (Fig. 5). The phase transformation itself takes place at the second stage. At this stage, oxygen near the island perimeter is captured into the new (oxide) phase. Simultaneously, surface atoms of the substrate are incorporated into the growing oxide lattice. We have not considered direct oxygen adsorption onto the oxide surface as contributing to the normal growth of the islands because the sticking coefficient S of oxygen on the oxide surface is usually substantially less than its value on the clean surface (by a factor of 10^3 for silicon[48]). The oxygen fluxes to the islands are composed of two terms: (i) The surface diffusion flux $j_1 = D\nabla c = D(\partial c/\partial r)$ at $r = R$—here, R is the island radius and $c(r)$ is a quasi-steady-state solution of the equation $\dot{c} = D\Delta c + QS(1-\Omega_a c) - \alpha c$ with the boundary conditions $c(r=R) = c'$ and $c(r \gg R) < \infty$, D is the surface oxygen diffusivity, $Q = p\{2\pi mT\}^{-1/2}$ is the oxygen flow from the gas phase, and α is the frequency of oxygen escape from the surface by desorption or/and diffusion into the bulk; and (ii) $j_2 = [QS(1-\Omega_a c') - \alpha c']l$ is the direct impingement flux, and l is the distance from the oxide perimeter where direct capture of oxygen atoms happens. The flux of oxygen incorporation into the island is[29] $j_3 = v(c' - c_R)$, where $c_R = c_f(1+\rho/R)$ is the equilibrium concentration[29] at $r = R$ when the rate of adatom incorporation into the island, v, is very high, i.e., $v \to \infty$, c_f is the equilibrium concentration of oxygen adatoms in the case of flat ($R \to \infty$) interface between oxide and adsorbed phase, $\rho = \sigma\Omega_a/T$ where σ is the "surface" tension coefficient. If we determine c' from $j_1 + j_2 = j_3$, then we obtain[27,28] the following expression for the rate of growth [$\dot{R} = \Omega_O(j_1 + j_2)$] of isolated oxide islands:

$$\dot{R} = \beta[(\tilde{Q} + \tilde{D})(1/R_c - 1/R)] , \tag{5}$$

where $\tilde{D} \equiv \Omega_O \rho c_f (D/L)[K_1(R/L)/K_0(R/L)]$; $\tilde{Q} \equiv \Omega_O \rho c_f (D/L)(1/L)$;

$$\beta = v\{v + (D/L)(1/L) + (D/L)[K_1(R/L)/K_0(R/L)]\}^{-1}$$

$$R_c = \rho_{c_f}/(\bar{c} - c_f) .$$

Here, Ω_O, Ω_a is the area of oxygen atom in oxide and adsorbate, respectively, $L \sim (D/\alpha)^{1/2}$ is the diffusion length, $\bar{c} = QS/(\alpha + QS\Omega_a)$ is the oxygen concentration far from the island, $K_i(x)$ is the modified Bessel functions of ith order, and R_c is the critical radius.

In order to provide oxide growth, it is necessary that the concentration of $\bar{c}$ be greater than the critical value of

TABLE I. Initial silicon oxidation as a first-order phase transition [1 represents island (cluster) formation, nonuniform oxidation with phase separation; 2 represents observation of critical pressure, exposure, or coverage; 3 represents coexistence of adsorbed and oxidelike phases during oxidation].

Reference	Techniques	Results 1	2	3
16	Electron microscopy		+	
10	SXPS		+	+
5	SXPS	+		
26	SXPS			+
7	XPS, molecular-beam scattering	+	+	
15	STM[a]	+	+	
11	SXPS	+		
8	XPS, UPS,[b] ARXPS[c]	+		
22	STM/STS[a]	+		+
12	XPS		+	+
19,20	XPS, ISS,[d] molecular-beam scattering	+	+	
23	STM[a]	+		
24	STM[a]	+		+
25	STM[a]	+		

[a]All STM images were taken at room temperature.
[b]Ultraviolet-photoemission spectroscopy.
[c]Angle-resolved x-ray-photoemission spectroscopy.
[d]Ion-scattering spectroscopy.

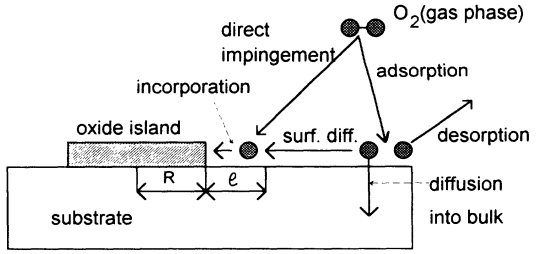

FIG. 5. Model of oxide island growth on the silicon surface.

c_f. By equating $\bar{c}$ and c_f, one may deduce the critical pressure:

$$p_c=\frac{\alpha c_f(2\pi mT)^{1/2}}{S(1-\Omega_a c_f)}=\frac{\alpha\theta_c(2\pi mT)^{1/2}}{S\Omega_a(1-\theta_c)} . \quad (6)$$

If the oxygen pressure is less than p_c, then the oxygen concentration will not exceed the critical value of c_f (or critical coverage of $\theta_c=c_f\Omega_a$), and as a result, an oxide phase will not be formed.

An increase in oxygen exposure results in an increase of the concentration of islands and their radii. This implies that we cannot consider the islands as isolated. They interact with each other in a diffusional way[49] via the field of adsorbed atoms. This interaction results in a decrease of steady-state oxygen adatom concentration (and consequently supersaturation) between the islands and therefore decreases island growth rate. Our consideration of island interaction differs to a certain extent from the direct ripening mechanism[29] studied for systems with mass conservation where the reduction of the initial supersaturation during island growth brings about the smaller island decomposition to maintain concentration gradient toward the bigger island. In our "open" system with constant oxygen flux to the surface from the gas phase, island interaction may not result in cluster decomposition. Instead, both the smaller and the bigger islands continue to grow but at a reduced rate as compared with the isolated islands considered above. The kinetics of interacting island growth was studied according to an the approach suggested in Ref. 28. The oxide coverage θ_{ox} is the second moment (I_2) of a distribution function $f(R,t)$ which is normalized to the island density of N, i.e., $\theta_{ox}=\pi I_2$, where $I_n=\int_0^\infty R^n f(R,t)dt$. On using the Fokker-Planck equation for the distribution function, we deduced a chain of equations for the moments, I_n. In the case of $R\gg R_c$, the chain could be unhooked.[27] As a result, we obtained a general expression for the oxide coverage of θ_{ox} in the form of an integral equation. It was possible to solve this equation analytically in the limits of $R\geq L$ and $R\leq L$. We analyzed all eight possible variants depending on the mechanism of oxygen delivery to the island (i.e., by way of surface diffusion: $\tilde{D}\gg\tilde{Q}$, or direct impingement: $\tilde{Q}\gg\tilde{D}$) and limiting stages of the oxidation (i.e., the oxidation rate is controlled either by oxygen delivery—$v\gg(D/L)$ or $v\gg(\alpha+Q\Omega_a S)l$—or by oxygen capture into the oxide phase in the vicinity on the island: $v\ll(D/L)$ or $v\ll(\alpha+Q\Omega_a S)l$. Each of these cases is characterized by a definite dependence of oxide coverage on the oxidation time, temperature, and pressure. Since the aim of this paper is to describe the initial oxidation of silicon, we do not present here all eight formulas for oxide coverage. It turns out (and we demonstrate it below in Sec. IV C) that the experimental data on initial silicon oxidation strongly imply the following mechanism. The oxide island grows via surface diffusion of oxygen ($\tilde{Q}<\tilde{D}$) and the oxidation rate is limited by oxygen incorporation into the island ($v<D/L$). Under these conditions, the oxide coverage is determined by

$$\theta_{ox}=\tanh^2\left[(\pi N)^{1/2}\Omega_O\frac{v}{\alpha+QS\Omega_a}\frac{S}{(2\pi mT)^{1/2}}(1-p_c/p)pt\right] . \quad (7)$$

C. The mechanism of oxide phase growth

We now show how the experimental results (the dependence of θ vs t, T, and p) can be explained on the basis of the theory outlined above. First, we discuss the dependence of oxide coverage on time. It should first be noted that in the experiment we record (Fig. 3) net oxygen coverage $\theta=n_O/n_s$ Eq. (1) as distinct from the oxide coverage θ_{ox} Eq. (7) that represents the fractional surface area covered by the oxide phase. Therefore, we used the formula $\theta=C_1\tanh^2\{C_2t\}$ instead of Eq. (7) in order to fit the experimental curves. The parameter of C_1 includes the coefficient of proportionality between θ and θ_{ox} that depends on the structure of the surface oxide and takes into account the contributions of oxygen atoms both adsorbed and diffused into subsurface into the value of θ. The theoretical curves compare quite favorably with the experimental ones (Fig. 3). According to the theory, the saturation of the $\theta(t)$ curves is due to the decrease of the surface area adsorbing oxygen during the process of island growth. Thus, the transition from so-called fast oxidation ($\theta<1$) to slow oxidation ($\theta>1$) (Fig. 3; Refs. 5 and 8) can be explained by the decrease of the effective surface area adsorbing oxygen. The value of C_1 increases with temperature. We believe that this occurs because of enhanced oxygen diffusion into the subsurface regions at higher temperatures. This is consistent with the O 1s spectrum [Fig. 2(c)], where we can see a small contribution of diffused oxygen species to the main peak corresponding to oxidelike oxygen.

The theory fails in fitting the higher-temperature curves 4 and 5. This can be explained as follows. According to Eq. (5), the critical pressure of p_c depends upon the temperature. A temperature increase at fixed oxygen pressure (p) gives rise to a small difference between p and p_c (curve 4). The temperature increase can even cause a transition from "passive" oxidation to "active" oxidation if the critical pressure becomes greater than the pressure p (curve 5, which exhibits an extremely low rate of oxygen uptake and the absence of a true Si^{4+} oxide state). In terms of the phenomenological theory of phase transitions, curve 4 represents oxide island growth with a very large critical radius and curve 5—negative critical radius (active oxidation), whereas the theoretical dependence of Eq. (6) was obtained under the assumption that $R\geq R_c$. It should be noted that oxide formation near the nucleation threshold (when the oxygen pressure is slightly greater than the critical pressure) is a separate

and quite different problem which demands special investigation.[50]

In order to discuss the temperature dependences, it is necessary to know the value of activation energies E_α and E_V. To reveal the value of E_α, we used the fact that the dependence of the critical pressure upon the temperature had the form $p_c \sim \exp(-E_\alpha/T)$ in accord with Eq. (6). The experimental result was found[16] to be $p_c = p_O \exp\{-(3.83\pm0.2)\ \text{eV/T}\}$ for Si(100); therefore, $E_\alpha = 3.83\pm0.2$ eV. As mentioned above, there are two channels by which oxygen can leave the surface: diffusion into subsurface or desorption of silicon monoxide. The activation energy of the former process is unknown to us. We suppose this value is less than the activation energy of the diffusion of interstitial oxygen in silicon crystal of 2.5 eV.[43–45] As to the activation energy of SiO desorption, it is equal to 3.5 ± 0.1 eV,[7] which fits with the value of 3.83 ± 0.2 eV within the error. Hence, we argue that oxygen escape from the surface is mainly due to SiO desorption. The experiment yielded an effective activation energy for oxidation of $E_a = -2.3$ eV [$K \sim \exp(-E_a/T)$]. The theoretical dependence, Eq. (7), results in $E_a = E_V - E_\alpha$. It follows that according to our theory the activation energy of oxygen capture into the island is $E_V = 1.53$ eV. It should be stressed that an activation energy of initial silicon [Si(100)] oxidation of 1.57 eV was recently calculated with the help of the atomic superposition and electronic-delocalization–molecular-orbital method;[51] silicon oxidation was treated in Ref. 51 as the transition of oxygen from an on-top adsorbed state into a short-bridge site between two silicon atoms in the first and the second surface layers. The observed decrease of oxidation rate with temperature increase is due to competition between two activated processes: oxygen capture into the island and oxygen escape from the surface with $E_\alpha > E_V$.

While exploring the effect of oxygen pressure on the kinetics of initial silicon oxidation at $T = 925$ K, Lutz *et al.*[8] found the universal dependence of oxygen coverage on exposure was destroyed in the pressure range of 7.6×10^{-7}–10^{-7} Torr, i.e., the coverage decreased with decreasing pressure at constant exposure $\epsilon = 100$ L (Fig. 6). This experimental result can be explained as follows. According to Eq. (7), the $\theta(\epsilon)$ dependence takes the form $\theta = C_1 \tanh^2[\text{const}\epsilon(1-p_c/p)]$, i.e., the coverage is determined not simply by oxygen exposure, but also by pressure. The solid line in Fig. 6 represents this theoretical dependence at $\epsilon = 100$ L, $\text{const} = 1.75\times10^{-2}$ L^{-1}, $p_c = 1.5\times10^{-7}$ Torr. The theory is valid for this range of oxide formation parameters, i.e., at $p > p_c$. For the opposite case, when $p < p_c$, only oxygen adsorption (described[20,52] by the Langmuir law) and SiO desorption occur. This means that the coverage is determined only by the exposure; this is actually observed at $p < p_c = 1.5\times10^{-7}$ Torr at $T = 925$ K (Fig. 6) and at $T = 300$ K as well. At $p \gg p_c$, the coverage depends simply on the exposure. However, the region of pressure above 7.6×10^{-7} Torr was not studied in Ref. 8. According to Eq. (7), we predict that these higher pressures should result in the universal dependence of the coverage

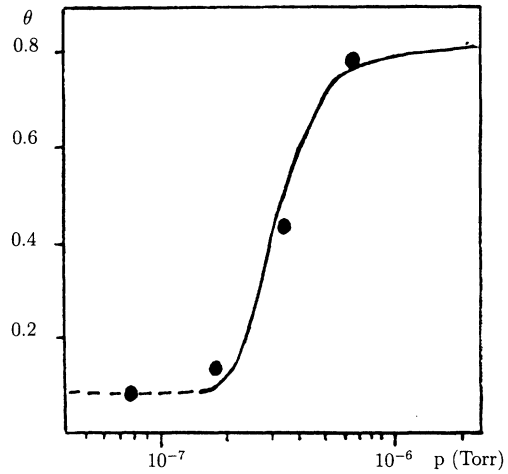

FIG. 6. The dependence of oxygen coverage upon the oxygen pressure at a constant exposure of $\epsilon = 100$ L. The experimental points are from Ref. 8. The solid line represents theoretical dependence. The dashed line illustrates schematically the behavior of oxygen coverage at $p < p_c$ when the oxide phase is not formed and only adsorption-desorption processes take place.

on exposure at $p \gg p_c$. The reason for the $\theta(\epsilon)$ anomaly at the intermediate pressures ($p \geq p_c$) is oxygen escape from the surface, i.e., nonconservation of the oxygen concentration on the surface.

It is impossible to establish a microscopic mechanism of oxygen atom capture into the island within the framework of the phenomenological theory. The proposed approach allows one only to determine whether a potential barrier (E_V) exists for oxygen to be incorporated into the island. Nevertheless, we can speculate somewhat with known information. The value of $E_V = 1.53$ eV is close to the value of the activation energy of silicon self-diffusion on the silicon surface $E_s = 1.51$ eV.[53] This is an indication that oxygen adatom capture into the island might be connected with a transition of the surface silicon atom from its crystalline lattice site. This transition is obviously accompanied by the Si-Si bond breaking off. According to Pauling,[54] the energy of a Si-Si bond in the silicon crystal is equal to 1.83 eV, which is close to 1.53 eV. The value of $E_V = 1.53$ eV appears to be comparable to the activation energy [$E_1 = 1.46$ eV for Si(100) (Ref. 55)] of silicon oxidation during the stage of linear growth. Following the Deal-Grove model,[55,56] the rate of thin-film growth during this stage is limited by the oxygen-silicon reaction at the Si-SiO_2 interface. The proximity of the activation energies of E_V and E_1 allows us to suggest that the mechanism of the transition of oxygen atoms into oxide is likely the same for both submonolayer oxide and thin (up to several hundred angstrom) oxide film. If so, the difference in silicon oxidation mechanism at $\theta < 1$ and at $\theta > 1$ exists only because of different means of oxygen delivery to the silicon surface: direct impingement at $\theta < 1$ and diffusion through the oxide at $\theta > 1$. Another argument favoring the equivalence of low- and high-coverage growth mechanisms is the observation reported in Ref. 12, where we find that oxide formation via a first-

order phase transition takes place not only during first monolayer growth ($\theta < 1$), but during second and third layers ($\theta > 1$) as well.

We cannot say anything about the mechanism of surface diffusion of oxygen adatoms on the silicon surface. Moreover, a picture of surface diffusion might be more complicated at certain oxidation conditions because of silicon surface etching (and consequently roughening) by SiO desorption. On the other hand, high-temperature oxygen adsorption on silicon does not bring about ordered adsorbate structures,[5] which implies a nonlocalized character of oxygen adsorption at these temperatures, i.e., oxygen adatoms are of sufficient mobility. Feltz, Memmert, and Behm[46] observed mobile species during high-temperature oxygen interaction with Si(111) by STM. They suggested that these species are due to either oxygen adatoms diffusing on the surface or vacancy diffusion. These facts do not contradict the suggested mechanism of submonolayer oxide growth, according to which oxygen delivery to the island is due to surface diffusion.

V. CONCLUSION

We have presented the results of an experimental and theoretical investigation of the kinetics of high-temperature oxide phase formation on the silicon surface during the island growth stage. The following kinetic features were observed in our real-time experiments: a coverage saturation at $\theta \sim 1$ with an increase in saturation value with increasing temperature, and a decrease in oxidation rate with temperature. On carrying out the measurements at elevated temperatures ($T > 1000$ K), we observed oxygen adatom diffusion into the subsurface. In order to explain both our and previously reported experimental results, we used a phenomenological first-order phase-transition theory. On the basis of the comparison of the theoretical results with the experimental data, a mechanism of submonolayer oxide growth was suggested. According to our mechanism, the interacting oxide islands grow via oxygen adatom surface diffusion, whereas the growth rate is limited by oxygen incorporation into the island at its perimeter within an average lifetime which is determined by oxygen desorption in the form of SiO. We also have accounted for available kinetic experimental results within the framework of the mechanism.

ACKNOWLEDGMENTS

The authors would like to thank Dr. Yu. N. Devyatko, Dr. V. N. Tronin, Dr. S. V. Rogozhkin, Professor E. Garfunkel, and Professor M. P. D'Evelyn for their helpful discussions, and Dr. P. A. Alexandrov for support and discussions.

[1]C. L. Claeys, R. F. De Keermaecker, and G. J. Declerck, in *The Si-SiO$_2$ System*, edited by P. Balk (Elsevier, Amsterdam, 1988).

[2]E. Irene, CRC Crit. Rev. Solid State Mater. Sci. **14**, 175 (1988).

[3]A. M. Stoneham, C. R. M. Grovenor, and A. Cerezo, Philos. Mag. B **55**, 201 (1987).

[4]N. F. Mott, S. Rigo, F. Rochet, and A. M. Stoneham, Philos. Mag. B **60**, 189 (1989).

[5]M. Tabe, T. T. Chiang, I. Lindau, and W. E. Spicer, Phys. Rev. B **34**, 2706 (1986).

[6]H. Ibach, H. D. Bruchmann, and H. Wagner, Appl. Phys. A **29**, 113 (1982).

[7]M. P. D'Evelyn, M. M. Nelson, and T. Engel, Surf. Sci. **186**, 75 (1987).

[8]F. Lutz, J. L. Bischoff, L. Kubler, and D. Bolmont, Phys. Rev. B **40**, 10 356 (1989); F. Lutz, L. Kubler, J. L. Bischoff, and D. Bolmont, Phys. Rev. B **40**, 11 747 (1989).

[9]P. J. Grunthaner, M. H. Hecht, F. J. Grunthaner, and N. M. Johnson, J. Appl. Phys. **61**, 629 (1987).

[10]G. Hollinger and F. J. Himpsel, Phys. Rev. B **28**, 3651 (1983).

[11]F. J. Himpsel, F. R. McFeely, A. Taleb-Ibrahimi, J. A. Yarmoff, and G. Hollinger, Phys. Rev. B **38**, 6084 (1988).

[12]V. D. Borman, E. P. Gusev, Yu. Yu. Lebedinskii, and V. I. Troyan, Phys. Rev. Lett. **67**, 2387 (1991).

[13]V. D. Borman, E. P. Gusev, Yu.Yu. Lebedinskii, A. P. Popov, and V. I. Troyan, Zh. Eksp. Teor. Fiz. **95**, 1378 (1989) [Sov. Phys. JETP **68**, 795 (1989)].

[14]The notation Si^{n+} means that a silicon atom placed at the center of a tetrahedron is bonded with n oxygen atoms. In accordance with the results of Chu and Fowler [A. X. Chu and W. B. Fowler, Phys. Rev. B **41**, 5061 (1990)], Si^{n+} states are connected with defects which determine electronic properties of the Si-SiO$_2$ system, for instance, with P_b centers (Si^{1+}, Si^{2+}) and E' centers (Si^{3+}).

[15]F. M. Leibsle, A. Samsavar, and T. C. Chiang, Phys. Rev. B **38**, 5780 (1988).

[16]F. W. Smith and G. Ghidini, J. Electrochem. Soc. **129**, 1300 (1982).

[17]J. J. Langer and J. Morrison, J. Appl. Phys. **33**, 2089 (1962).

[18]T. Engel, Surf. Sci. Rep. **18**, 91 (1993).

[19]J. R. Engstrom, D. J. Bonser, M. M. Nelson, and T. Engel, Surf. Sci. **256**, 317 (1991).

[20]J. R. Engstrom, D. J. Bonser, and T. Engel, Surf. Sci. **268**, 238 (1992).

[21]F. Rochet, S. Rigo, M. Froment, C. d'Anterroches, C. Maillot, H. Roulet, and G. Dufour, Adv. Phys. **35**, 2356 (1986).

[22]Ph. Avouris and In-Whan Lyo, Surf. Sci. **242**, 1 (1991); Ph. Avouris, In-Whan Lyo, and F. Bozso, J. Vac. Sci. Technol. B **9**, 424 (1991).

[23]M. Udagawa, M. Niwa, and I. Sumita, Jpn. J. Appl. Phys. **32**, 282 (1993).

[24]J. Seiple, J. Pecquet, Z. Meng, and J. P. Pelz, J. Vac. Sci. Technol. A **11**, 1649 (1993).

[25]U. Neuwald, H. E. Hessel, A. Feltz, U. Memmert, and R. J. Behm, Appl. Phys. Lett. **60**, 1307 (1992).

[26]G. Hollinger, J. F. Morar, F. J. Himpsel, G. Hughes, and J. L. Jordan, Surf. Sci. **168**, 609 (1986).

[27]V. D. Borman, E. P. Gusev, Yu. N. Devyatko, Yu. Yu. Lebedinskii, S. V. Rogozkin, V. N. Tronin, and V. I. Troyan, (unpublished).

[28]V. D. Borman, E. P. Gusev, Yu. N. Devyatko, Yu. Yu. Lebedinskii, S. V. Rogozkin, V. N. Tronin, and V. I. Troyan, Poverkhost' **8**, 22 (1990). [Engl. Transl. in Phys. Chem. Mech. Surf. **6**, 1845 (1991)].

[29]M. Zinke-Allmang, L. C. Feldman, and M. H. Grabow, Surf. Sci. Rep. **16**, 377 (1992).

[30]P. H. Holloway and J. B. Hudson, Surf. Sci. **43**, 123 (1974).

[31]J. A. Venables and G. D. T. Spiller, *Surface Mobilities on Solid Materials*, edited by Vu Thien Binh (Plenum, New York, 1983), p. 341.

[32]E. P. Gusev and A. P. Popov, Surf. Sci. **248**, 241 (1991).

[33]B. Carriere, A. Chouiyakh, and B. Lang, Surf. Sci. **126**, 495 (1983).

[34]P. Pianetta, I. Lindau, C. M. Garner, and W. E. Spicer, Phys. Rev. Lett. **37**, 1166 (1976).

[35]Cross section of Si 2*p* core level was found (Ref. 11) to differ for the various oxidation states (Si^{n+}) in a photon energy range of 120–400 eV. We have no information on this effect for the photon energy of 1254 eV involved. Also, only the Si^0 (substrate) state cross section is required for the oxygen coverage calibration.

[36]J. H. Scofield, J. Electron Spectrosc. Relat. Phenom. **8**, 129 (1976).

[37]M. F. Hochella, Jr. and A. H. Carim, Surf. Sci. **197**, L260 (1988).

[38]P. R. Norton, P. E. Bindner, and T. E. Jackman, Surf. Sci. **175**, 313 (1986).

[39]F. J. Grunthaner, P. J. Grunthaner, R. P. Vasquez, B. F. Lewis, J. Maserjian, and A. Madhukar, Phys. Rev. Lett. **43**, 1683 (1979).

[40]P. Morgen, U. Hofer, W. Wurth, and E. Umbach, Phys. Rev. B **39**, 3720 (1989).

[41]A. Namiki, K. Tanimoto, T. Nakamura, N. Ontake, and T. Suzaki, Surf. Sci. **222**, 530 (1989).

[42]More recent STM experiments (E. Garfunkel, private communications) show that the initial stage of oxygen interaction with Si(111) is more complicated with up to five oxygen sites on the surface, as followed from their different brightnesses in STM images.

[43]M. Stavola, J. R. Patel, L. C. Kimerling, and P. E. Freeland, Appl. Phys. Lett. **42**, 73 (1983).

[44]S. Tong Lee and D. Nichols, Appl. Phys. Lett. **47**, 1001 (1985).

[45]J. C. Mikkelsen, Jr., Appl. Phys. Lett. **40**, 336 (1982).

[46]A. Feltz, U. Memmert, and R. J. Behm, Chem. Phys. Lett. **192**, 271 (1992).

[47]Silicon oxide growth in the form of two-dimensional islands was observed recently (Ref. 25) by STM during native oxidation. However, we should mention that in some cases (Refs. 22–25) oxide islands do not have regular circular form as it was postulated in our model. The deviation in island form from the two-dimensional disk makes theoretical consideration very difficult but does not affect the main results.

[48]P. Gupta, C. H. Mak, P. A. Coon, and S. M. George, Phys. Rev. B **40**, 7739 (1989).

[49]L. A. Maximov and A. I. Ryazanov, Fiz. Metal. Metaloved. **41**, 284 (1976).

[50]V. D. Borman, E. P. Gusev, Yu. N. Devyatko, V. N. Tronin, and V. I. Troyan, Surf. Sci. **301**, L239 (1994).

[51]X. M. Zheng and P. V. Smith, Surf. Sci. **232**, 6 (1990).

[52]M. R. Baklanov, V. N. Kruchinin, S. M. Repinsky, and A. A. Shklyaev, React. Solids **7**, 1 (1989).

[53]P. M. Agrawal, L. W. Raff, and D. L. Thompson, J. Chem. Phys. **91**, 6463 (1989).

[54]L. Pauling, *The Nature of the Chemical Bond* (Cornell University Press, Ithaca, NY, 1960).

[55]A. Atkinson, Rev. Mod. Phys. **57**, 437 (1985).

[56]B. E. Deal and A. S. Grove, J. Appl. Phys. **36**, 3770 (1965).

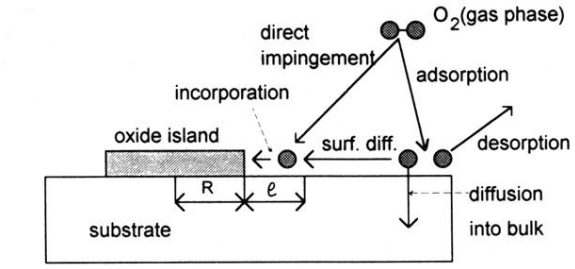

FIG. 5. Model of oxide island growth on the silicon surface.